Journal of Alloys and Compounds 488 (2009) 479–481

Contents lists available at ScienceDirect

Journal of Alloys and Compounds

journal homepage: www.elsevier.com/locate/jallcom

Thermodynamic modeling of the Sc_2O_3–MgO phase diagram

Sung S. Kim*

School of Materials Science and Engineering, Hongik University, Jochiwon 339-701, Republic of Korea

ARTICLE INFO

Article history:
Received 15 October 2008
Received in revised form 1 September 2009
Accepted 6 September 2009
Available online 11 September 2009

Keywords:
Phase diagram
Thermodynamic modeling
Metastable miscibility gap
Sc_2O_3–MgO

ABSTRACT

The Sc_2O_3–MgO system consists of one liquid and two solid solutions. A relatively simple approach is used to model the solution phases, which are treated as the regular and the sub-regular solutions of the end-members. The solution parameters are derived from the phase equilibrium data. The thermodynamic calculations using the model allow the determination of the liquidus, solidus, solvus, and metastable liquid miscibility gap. Also the lattice stabilities of the components are evaluated.

1. Introduction

The heat engines in the jet aircraft and the power generators should work at higher temperatures to increase their thermal efficiency. Thus, there is strong need to develop a material that remains stable at very high temperatures. The ceramic eutectics are potential candidates as reinforcement fibers for ceramic and intermetallic matrix composites in the structural applications [1–3]. The Sc_2O_3–MgO eutectic might be useful as a promising high-temperature structural ceramic material. Sc_2O_3 is a cubic crystal bixbyite-structure described as a defect fluorite structure in which only six of the eight corners of the anionic cubes are occupied. The unit cell consists of 16 formula units. Thus there are 32 Sc-ions in the unit cell, 24 occupy the site with C_2 symmetry, 8 occupy the site with C_{3i} symmetry. MgO has the NaCl-type structure, where both cations and anions have octahedral coordination of six other ions.

There are several experimental works on the phase equilibria in the Sc_2O_3–MgO system [4–7]. Lopato et al. [7] investigated phase equilibria in the Sc_2O_3–MgO system in the temperature range 1500–2300 °C. To determine the solvus curve, Mo encapsulated specimens were annealed and quenched and then their lattice constants were measured with X-ray diffraction. The liquidus and solidus curves were also investigated using high-temperature DTA with temperature accuracy ±20 °C. The eutectic point was determined at 55 mol% MgO and 2260 °C. The eutectic phases consisted of the Sc_2O_3-rich phase with 30 mol% MgO and the MgO-rich phase with 85 mol% Sc_2O_3. Muller-Buschbaum [5] found the compound $MgSc_2O_4$, which was prepared above 2000 °C. However, Lopato et al. [7] regarded it as a mixed oxide since the metal ions in the $MgSc_2O_4$ are distributed statistically among the metal positions. So far, no compound has been reported in the Sc_2O_3–MgO system.

In the Sc_2O_3–MgO phase diagram from Lopato et al. [7], most of the liquidus and the solidus curves were not determined due to the high melting points of the components. Until now, there are not many high-temperature experimental data in the Sc_2O_3–MgO system available in the literatures. In the present work, a thermodynamic modeling of the Sc_2O_3–MgO phase diagram was performed by using the regular and the sub-regular solution models. A tentative phase diagram is suggested by calculating the liquidus, solidus, solvus, and metastable liquid miscibility gap. Also the lattice stabilities of each component were evaluated.

2. Thermodynamic methodology

Numerous analytical thermodynamic models have been proposed to account for the thermodynamic behavior of various systems [8]. Kim et al. [9–14] have described the solution phases of the binary systems with a simple model. The present system shows a simple eutectic reaction with no intermediate phases. In the present work, therefore, the regular and the sub-regular solution models were applied to describe the solution phases. Pure components Sc_2O_3 and MgO have the bixbyite and the halite structures over the temperature range from room temperature to their melting points, respectively. The Gibbs free energies of liquid (L) phase in the *i*–*j* system is given by

$$G^{L} = (1-x)\Delta G_i^{STD\to L} + x\Delta G_j^{STD\to L} + RT[(1-x)\ \ln(1-x) + x\ \ln x] + x(1-x)[A_0^{L} + A_1^{L}(1-2x)] \quad (1)$$

* Tel.: +82 41 860 2580; fax: +82 41 862 2774.
E-mail address: sungkim@wow.hongik.ac.kr.

0925-8388/$ – see front matter © 2009 Elsevier B.V. All rights reserved.
doi:10.1016/j.jallcom.2009.09.014

where, x is the mole fraction of component j, $\Delta G_i^{\mathrm{STD}\to\mathrm{L}}$ and $\Delta G_j^{\mathrm{STD}\to\mathrm{L}}$ are the Gibbs free energy changes from the standard state (STD) to the L phase for pure components i and j, respectively, and ${A_n}^{\mathrm{L}}$'s are the n-th interaction parameters of the L phase. Similar equations can be written for other solution phases with the superscripts replaced by B and H for the bixbyite and the halite phases, respectively.

At constant temperature and pressure, equilibrium occurs when the partial molar Gibbs free energies of each component are equal in all phases. The partial molar Gibbs free energies of components i and j for the liquid phase are given by

$$\overline{G}_i^{\mathrm{L}} = \Delta G_i^{\mathrm{STD}\to\mathrm{L}} + RT\ \ln(1-x) + x^2[A_0^{\mathrm{L}} + A_1^{\mathrm{L}}(3-4x)] \quad (2a)$$

$$\overline{G}_j^{\mathrm{L}} = \Delta G_j^{\mathrm{STD}\to\mathrm{L}} + RT\ \ln x + (1-x)^2[A_0^{\mathrm{L}} + A_1^{\mathrm{L}}(1-4x)] \quad (2b)$$

Similar equations can be written for other solution phases.

To model phase diagrams, basic physical data for the components such as heat capacity, melting point, heat of fusion, and the lattice stability are required. The heat capacity data of the solid and liquid phases, however, are available for only a few oxides and are sometimes inaccurate [15,16]. There exist some heat capacity data of only solid phase for Sc_2O_3 and MgO [17]. Therefore, in the present work, the difference in the heat capacities of the liquid and solid phases were neglected to calculate the interaction parameters of the solid and liquid solution phases. The melting temperatures of pure Sc_2O_3 and MgO are taken as 2470 and 2832 °C [17], respectively. The heat of fusion for Sc_2O_3 is chosen as 96.30 kJ/mol [18] and that for MgO as 77.82 kJ/mol [17].

There exist no pressure vs. temperature diagrams for Sc_2O_3 and MgO to calculate their lattice stabilities between the bixbyite and halite phases. Therefore, the method used by Kaufman et al. [19–21] was used to estimate the metastable melting points. The extension of B/L liquidus and solidus trajectory to the pure component MgO corresponds to $T_{\mathrm{MgO}}^{\mathrm{B}\to\mathrm{L}}$, which is the metastable melting point of bixbyite MgO. Similarly, extension of the H/L trajectory to pure Sc_2O_3 yields the metastable melting point of halite Sc_2O_3, $T_{\mathrm{Sc_2O_3}}^{\mathrm{H}\to\mathrm{L}}$. However, there have been no binary phase diagrams available in the literature that consist of Sc_2O_3 (or MgO) and a component with halite (or bixbyite) phase. Therefore, the present trajectories were evaluated by using the eutectic reaction data [7] and by referring to the trajectories of liquidus and solidus curves that were derived from a regular solution model [22]. The metastable melting points were estimated as $T_{\mathrm{MgO}}^{\mathrm{B}\to\mathrm{L}} = 2280$ °C and $T_{\mathrm{Sc_2O_3}}^{\mathrm{H}\to\mathrm{L}} = 2029$ °C.

The interaction parameters of the liquid and solid phases should satisfy the equilibrium conditions such as the liquidus, solidus, and solvus curves. The present modeling was carried out through the following optimization procedure. First, the interaction parameter for the bixbyite phase was varied keeping a fixed one for the halite phase to fit the solvus below the eutectic temperature. Second, the interaction parameter of the halite phase was varied using the newly calculated interaction parameter of the bixbyite phase. These procedures were then repeated until a satisfactory solvus had been achieved. Finally, the interaction parameter of the liquid phase was determined using the interaction parameters of the bixbyite and halite phases to satisfy the experimental data above the eutectic temperature.

3. Results and discussion

The calculated phase diagram is presented in Fig. 1, together with other experimental data. The optimized interaction parameters of liquid, bixbyite, and halite are ${A_0}^{\mathrm{L}} = 252.30 - 0.10T$, ${A_1}^{\mathrm{L}} = 14.00$, ${A_0}^{\mathrm{B}} = 125.92 - 0.042T$, and ${A_0}^{\mathrm{H}} = 91.85 - 0.241T$ kJ/mol, respectively. From these parameters, a eutectic point is determined at 53.6 mol% MgO and 2260 °C. At the eutectic temperature,

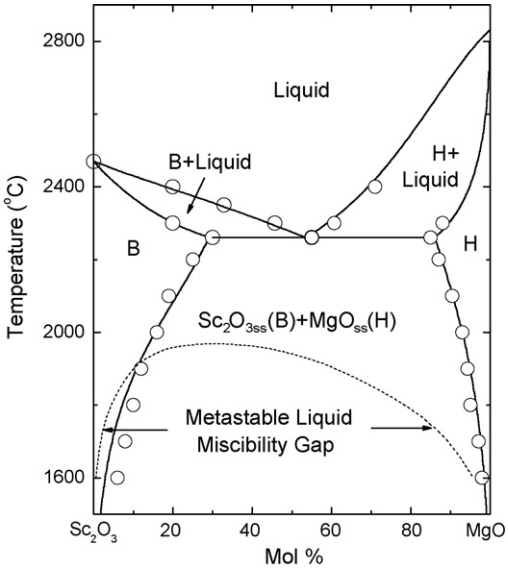

Fig. 1. Calculated phase diagram of Sc_2O_3–MgO system (O: [7]).

the bixbyite phase contains the highest solubility of 29.2 mol% MgO and the halite phase contains that of 14.01 mol% Sc_2O_3. The present calculated solidus, liquidus, and solvus curves are in good agreement with the experimental data (circles in Fig. 1) [7]. Both the experimental and the present calculated liquidi in the MgO side are S-shaped. Therefore, a metastable liquid miscibility gap is expected in the lower temperature and calculated in Fig. 1. Its critical point is located at 30.3 mol% MgO and 1973 °C. The metastable liquid immiscibility in the present system might lead to form the metastable mixed oxide $MgSc_2O_4$ above 2000 °C [5].

From the optimization procedure, the metastable entropies of fusion were estimated as $\Delta S_{\mathrm{Sc_2O_3}}^{\mathrm{H}\to\mathrm{L}} = 25.11$ J/mol K and $\Delta S_{\mathrm{MgO}}^{\mathrm{B}\to\mathrm{L}} = 30.06$ J/mol K. By using the entropies of fusion $\Delta S_{\mathrm{Sc_2O_3}}^{\mathrm{B}\to\mathrm{L}} = 35.11$ J/mol K and $\Delta S_{\mathrm{MgO}}^{\mathrm{H}\to\mathrm{L}} = 25.06$ J/mol K, the entropy changes between the bixbyite and halite phases are obtained as

$$\Delta S_{\mathrm{Sc_2O_3}}^{\mathrm{B}\to\mathrm{H}} = \Delta S_{\mathrm{Sc_2O_3}}^{\mathrm{B}\to\mathrm{L}} - \Delta S_{\mathrm{Sc_2O_3}}^{\mathrm{H}\to\mathrm{L}} = 10.0\,\mathrm{J/mol\,K}$$

and

$$\Delta S_{\mathrm{MgO}}^{\mathrm{B}\to\mathrm{H}} = \Delta S_{\mathrm{MgO}}^{\mathrm{B}\to\mathrm{L}} - \Delta S_{\mathrm{MgO}}^{\mathrm{H}\to\mathrm{L}} = 5.0\,\mathrm{J/mol\,K}.$$

The phase transformations due to the pressure decrease or the temperature increase become more open structure and make a cation adapting a lower coordination number [23]. The change from the bixbyite to the halite structure makes the coordination number of cations unchanged but becomes more open structure considering the bixbyite-structure as the defected fluorite structure. Therefore, the entropy increase in the present work is reasonable. Since the bixbyite-structure is more complicated than the fluorite structure, the smaller entropy changes from the bixbyite to the halite structure are reasonably compared to those from the fluorite (F) to the halite structure in the CeO_2–CoO system: $\Delta S_{\mathrm{CeO_2}}^{\mathrm{F}\to\mathrm{H}} = 10.0$ J/mol K and $\Delta S_{\mathrm{CoO}}^{\mathrm{F}\to\mathrm{H}} = 14.0$ J/mol K [14].

From the metastable melting points estimated as $T_{\mathrm{Sc_2O_3}}^{\mathrm{H}\to\mathrm{L}} = 2029$ °C and $T_{\mathrm{MgO}}^{\mathrm{B}\to\mathrm{L}} = 2280$ °C, the enthalpy changes between the bixbyite and halite phases are given as

$$\Delta H_{\mathrm{Sc_2O_3}}^{\mathrm{B}\to\mathrm{H}} = \Delta H_{\mathrm{Sc_2O_3}}^{\mathrm{B}\to\mathrm{L}} - \Delta H_{\mathrm{Sc_2O_3}}^{\mathrm{H}\to\mathrm{L}} = \Delta H_{\mathrm{Sc_2O_3}}^{\mathrm{B}\to\mathrm{L}} - T_{\mathrm{Sc_2O_3}}^{\mathrm{H}\to\mathrm{L}}\,\Delta S_{\mathrm{Sc_2O_3}}^{\mathrm{H}\to\mathrm{L}}$$
$$= 38496.78\,\mathrm{J/mol}$$

and

$$\Delta H_{MgO}^{H\to B} = \Delta H_{MgO}^{H\to L} - \Delta H_{MgO}^{B\to L} = \Delta H_{MgO}^{H\to L} - T_{MgO}^{B\to L}\Delta S_{MgO}^{B\to L} = 1076.82\,\text{J/mol}.$$

Therefore, the lattice stabilities of Sc_2O_3 and MgO between the bixbyite and halite structures were estimated as $\Delta G_{Sc_2O_3}^{B\to H} = 38496.78 - 10.0T(\text{J/mol})$ and $\Delta G_{MgO}^{H\to B} = 1076.82 + 5.0T(\text{J/mol})$, respectively.

4. Conclusion

A phase diagram of Sc_2O_3–MgO system was modeled thermodynamically. The excess Gibbs energies of the solution phases were described on the basis of the regular and the subregular solutions. The optimized interaction parameters of the liquid, bixbyite, and halite phases were ${}^0L^L = 252.30 - 0.10T$, ${}^1L^L = 14.00$, ${}^0L^B = 125.92 - 0.042T$, and ${}^0L^H = 91.85 - 0.241T$ kJ/mol, respectively. The solidus, liquidus, and solvus curves were calculated reasonably and the metastable liquid miscibility gap was estimated. Also, the lattice stabilities of the Sc_2O_3 and MgO between the bixbyite and halite phases were evaluated.

Acknowledgement

This work was supported by the 2007 Hongik University Research Fund.

References

[1] M. Omoru, T. Isobe, T. Hirai, J. Am. Ceram. Soc. 83 (2000) 2878.
[2] Y. Waku, N. Nakagawa, T. Wakamoto, H. Ohtsybo, K. Shimizu, Y. Kohtoku, Nature 389 (1997) 49.
[3] T.-I. Mah, M.D. Petry, J. Am. Ceram. Soc. 75 (1992) 2006.
[4] S.G. Tresvyatskii, L.M. Lopato, Z.A. Yaremenko, Porosh. Met. 4 (1964) 29.
[5] H.K. Muller-Buschbaum, Z. Anorg, Allg. Chem. 343 (1966) 113.
[6] L.M. Lopato, A.A. Ogorodnikova, A.V. Shevchenko, Dopov. Akad. Nauk Ukr. RSR, Ser. B: Geol., Khim. Biol. Nauki 32 (1970) 1106.
[7] L.M. Lopato, A.A. Ogorodnikova, A.V. Shevchenko, Inorg. Mater. (Engl. Transl.) 8 (1972) 1111.
[8] H.L. Lukas, S.G. Fries, B. Sundman, Computational Thermodynamics—The Calphad Method, Cambridge University Press, UK, 2007.
[9] S.S. Kim, J. Am. Ceram. Soc. 78 (1995) 1101.
[10] S.S. Kim, T.H. Sanders Jr., J. Am. Ceram. Soc. 84 (2001) 1881.
[11] S.S. Kim, J.Y. Park, T.H. Sanders Jr., J. Alloys Compd. 321 (2001) 84.
[12] S.S. Kim, T.H. Sanders Jr., J. Am. Ceram. Soc. 86 (2003) 1947.
[13] S.S. Kim, T.H. Sanders Jr., Z. Metallkd. 94 (2003) 390.
[14] S.S. Kim, J. Alloys Compd. 390 (2005) 223.
[15] M. Binnewies, E. Milke, Thermochemical Data of Elements and Compounds, 2nd ed., Wiley-VCH, Wenheim, 2002.
[16] C.G. Bergeron, S.H. Risbud, Introduction to Phase Equilibria in Ceramics, American Ceramic Society, Columbus, OH, 1984.
[17] O. Knacke, O. Kubaschewski, K. Hesselmann (Eds.), Thermochemical Properties of Inorganic Substances, 2nd ed., Springer-Verlag, New York, 1991.
[18] G.V. Samsonov (Ed.), The Oxide Handbook, 2nd ed., IFI/PLENUM, New York, 1982.
[19] L. Kaufman, H. Bernstein, Computer Calculation of Phase Diagrams, Academic Press, New York, 1970.
[20] L. Kaufman, H. Nesor, CALPHAD 2 (1978) 35.
[21] L. Kaufman, CALPHAD 3 (1979) 27.
[22] A.D. Pelton, W.T. Thompson, Prog. Solid State Chem. 10 (1975) 119.
[23] F.D. Bloss, Crystallography and Crystal Chemistry: An Introduction, Rinehart and Winston, New York, 1971.